JOURNAL OF CATALYSIS **176,** 387–394 (1998)
ARTICLE NO. CA982037

Characterisation of Spent Fluid Catalytic Cracking Catalysts by Nuclear Microprobe Techniques

D. A. Jacobs,* G. C. Smith,†,[1] R. D. Vis,* and A. F. H. Wielers†,[2]

*Faculty of Physics and Astronomy, Vrije Universiteit, Amsterdam, The Netherlands; and †Shell Research and Technology Centre Amsterdam, P.O. Box 38000, 1030 BN Amsterdam, The Netherlands

Received November 10, 1997; revised January 28, 1998; accepted January 28, 1998

The nuclear microbeam analysis techniques of proton-induced X-ray emission (PIXE) and nuclear reaction analysis (NRA) have been used to probe the distribution of carbon and other elements in used fluid catalytic cracking catalyst particles. The catalyst was sampled from the stripper standpipe in one of Shell's commercial riser FCC units processing feedstocks containing up to 4 wt% Conradson carbon residue (CCR). PIXE and NRA gave quantitative information on the metal and carbon distributions. Samples were embedded in waterglass ($Na_2O \cdot SiO_2$) to overcome the problem of carbon contamination from conventional embedding materials. Elemental line scans and images were obtained with a spatial resolution of a few microns and sufficient sensitivity to allow quantification of all elements of interest. Correlations were found between the spatial distribution of Ti, V, and, to a lesser extent, Fe. Ni was found to be confined to the outermost 10 μm or so of each particle. The degree of correlation appeared to reduce with particle age. Despite the high CCR content of the feedstock, it was found that carbon was uniformly distributed through the particles, indicating that even the bulkier molecules present in the feed are cracked on the external surface of the FCC particle. © 1998 Academic Press

1. INTRODUCTION

Carbon, in the form of coke, plays a significant role in the deactivation of hydrocarbon cracking catalysts. The mechanism of coke deactivation processes is not fully understood, but it may involve poisoning of, or blocking of access to, active sites on the catalyst. The coke is removed during high temperature oxidative regeneration of the catalyst; however, the hydrothermal conditions prevailing in the regenerator irreversibly degrade the catalyst performance through structural and/or chemical changes. To understand the coke deactivation mechanism during fluid catalytic cracking, and thereby offer suggestions for remediation, it is essential to have improved characterisation of the coke deposits on a "real life" FCC catalyst. However, individual fluidised catalytic cracking (FCC) catalyst particles are small (typically 50–100 μm in diameter) and have a complex structure with silica, clay, alumina, and zeolite phases. Consequently, the microcharacterisation of the nature and distribution of coke within FCC particles is an intricate problem and it has proved difficult to use conventional electron and other microscopy techniques to give the required information. Difficulties arise as a result of the low concentrations involved (carbon may typically be found at around 1 wt% in used catalysts) and the requirement for high spatial resolution (the zeolite particles have sizes in the range 0.1–3 μm). Further, in the FCC process a small proportion of the catalyst particles are regularly replaced. There is consequently a spread in the age distribution of the individual catalyst particles.

Instrumental methods for FCC catalyst characterisation have been reviewed by Peters (1), among others. A large number of techniques has been applied to these materials, including diffractive, thermal, spectroscopic, and physical methods, as well as surface analysis and microscopic imaging techniques (1). Secondary ion mass spectrometry (SIMS) has successfully been used to identify the presence and relative distribution of poisoning metals such as Fe, Ni, and V in FCC catalyst particles (2–4). X-ray photoelectron spectroscopy (XPS) has been used to give information on the oxidation state of these elements (5, 6). Auger electron spectroscopy (AES) has been applied to the characterisation of ex-refinery equilibrium FCC particles (7) and used to identify the presence of increased levels of carbon on the outer surface. Investigations of the local structure of coke within zeolites have been performed by electron microscopy (8); however, in that work it was necessary to load the catalyst artificially with unrealistically high carbon levels. Although the nature of the coke on industrial FCC samples has been investigated with conventional bulk analytical techniques (9) to our knowledge, no work on carbon distributions within FCC particles extracted directly from industrial plant has been reported.

For the work presented here samples were extracted from the stripper standpipe during operation of the FCC

[1] Author for correspondence. Present address: Shell Research and Technology Centre Thornton, P.O. Box 1, Chester, CH1 3SH, United Kingdom. E-mail: g.c.smith@msmail.trctho.simis.com.

[2] Present address: Société Couronnaise de Raffinage, 76650 Le Petit Couronne, France.

0021-9517/98 $25.00
Copyright © 1998 by Academic Press and Shell International Chemicals B.V.
All rights of reproduction in any form reserved.

plant. They are therefore equilibrium samples taken just before the regeneration stage and are truly representative of carbon-containing FCC catalyst particles; the carbon being formed during the cracking and stripping processes. The regenerator of the particular FCC unit from which samples were taken operates in partial combustion mode. Residence time in the riser section is between 5 and 10 s, and the operating temperature is approximately 520°C. The reactor and stripper residence time is 2–5 min, and the amount of steam in the stripper corresponds to a partial pressure of approximately 0.1–0.2 bar. On average, the as-sampled catalyst particles had a composition of 24.0 wt% Si, 21.4 wt% Al, 0.94 wt% Ti, 0.45 wt% Fe, 0.45 wt% V, 0.37 wt% Ni, and 1.24 wt% C. After regeneration, the C level was <0.2 wt% on average.

To prepare cross sections or slices of catalyst particles for microscopic techniques, they must first be fixed by embedding them. FCC catalyst particles are usually highly porous; therefore the embedding methods using polymeric materials which are routinely applied in electron and optical microscopy may introduce carbon at a much higher level than the amount originally present in the catalyst. This would effectively prohibit a combined spectroscopic and microscopic characterisation of the original carbonaceous compounds. To overcome this problem, samples were embedded in waterglass (sodium silicate, $Na_2O \cdot SiO_2$). Using a thin layer technique, followed by careful polishing, suitable samples for analysis were prepared.

In view of the low levels of carbon in the samples, surface sensitive techniques such as AES or imaging XPS, with their sensitivity to adventitious carbonaceous contamination, are very difficult to use for the determination of intra-particle carbon distributions. Electrostatic charging of these insulating materials poses an additional problem. Similar comments apply to SIMS, which has the added disadvantage that the results cannot easily be quantified. In principle, electron probe microanalysis (EPMA) carried out with a thin-window or windowless detector could be used to tackle this problem, but EPMA instruments generally operate at rather poor vacua and substantial carbon deposition on the specimen surface may occur during analysis. For these reasons, we have investigated the potential benefits of the application of nuclear microbeam techniques to the analysis of used FCC catalyst particles.

The nuclear beam techniques of micro-PIXE (proton induced X-ray emission) and NRA (nuclear reaction analysis) can give information on elemental distributions, including carbon, with high sensitivity (10). Micro-PIXE is the nuclear beam equivalent of EPMA. A focused beam of energetic protons is directed at the sample surface and the spectrum of emitted X-rays is used to give information on the elemental composition of the sample. In comparison with EPMA, the cross sections for X-ray production are similar, but the background is much lower, resulting in much improved detection limits. In NRA the emission of characteristic nuclear particles following nuclear reaction induced by the impact of (in this case) a deuteron beam is used as a measure of the amount of a specific element that is present. In our work, the NRA technique was used to give information on the distribution of carbon, while other elements with atomic number greater than 11 were probed by micro-PIXE.

In the following sections of this paper we describe the sample preparation and measurement techniques in more detail and discuss the results of averaged analyses, linescans, and element distribution images.

2. EXPERIMENTAL METHODS

2.1. Sample Preparation

As an alternative for the conventional embedding materials, the potential of embedding in waterglass was explored. Waterglass is a low viscosity solution of sodium silicate ($Na_2O \cdot SiO_2$) which, when poured as a thin film on a substrate, dries readily, leaving a transparent solid.

The preparation procedure was as follows. A thin film of waterglass was placed on a quartz substrate and several FCC catalyst particles were distributed on it. Due to the low viscosity of the waterglass and the capillary forces, the catalyst particles are wetted rather well. After the water had evaporated, the process of adding another thin liquid film and letting it dry was repeated several times. This was necessary because the volume of the waterglass changes considerably during water evaporation giving rise to stresses and cracks which otherwise prevent satisfactory polishing of the samples. As a final step, the samples were polished manually to expose cross sections of the catalyst particles and their condition was checked using polarisation contrast optical microscopy. Figure 1 shows a schematic view of the final sample structure and Fig. 2 shows an optical micrograph of two embedded and polished particles.

2.2. Nuclear Microprobe Analysis Techniques

PIXE and NRA analyses were performed using the nuclear microprobe facility of the Vrije Universiteit,

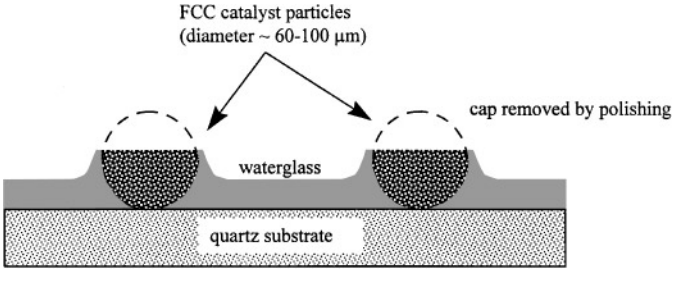

FIG. 1. Schematic drawing showing section of FCC catalyst particle after embedding in waterglass and polishing.

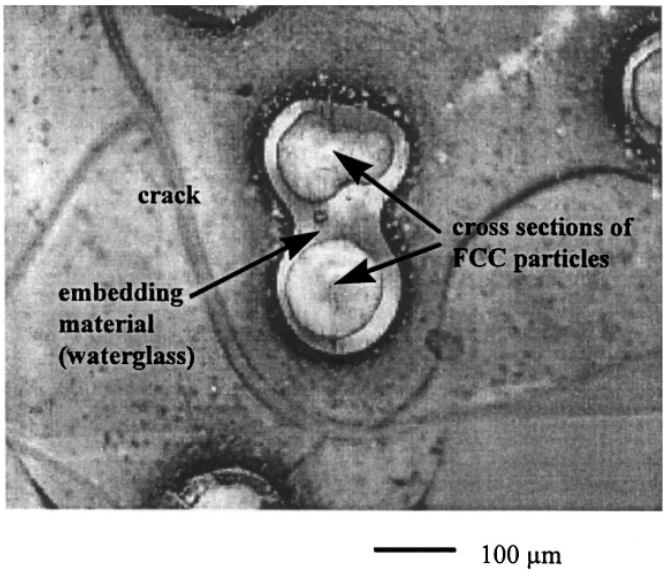

FIG. 2. Optical micrograph of embedded FCC catalyst particles.

Amsterdam (11). This facility incorporates an Alphatross charge exchange ion source and a 1.7 MV NEC 5SDH-2 electrostatic Pelletron accelerator to produce a proton or deuteron beam of up to 3.4 MeV energy. The beam may be focused into a spot of minimum diameter approximately 1 μm and scanned over a range of up to 150 μm. A high purity Ge detector is used for the detection of X rays produced in the PIXE process, and an annular surface barrier detector is used for the detection of particles produced by NRA.

2.2.1. Particle induced X ray emission (PIXE). To optimise the cross section, PIXE was performed using a 2.5 MeV proton beam at a current of approximately 200 pA, resulting in a current density of approximately 20 Am^{-2}. Under these conditions, useful data could be acquired in 10 min. At 2.5 MeV beam energy, the microprobe can run with currents up to 1000 pA; however, this was limited to 200 pA to avoid sample damage. The PIXE information depth depends on the beam energy and the sample, but under the conditions used here it is typically 10 μm. Quantification of the PIXE data was achieved using the known composition of the waterglass embedding material as a standard. Quantification calculations were performed using the Gupix software developed at Guelph, Canada (12). Further information on the PIXE technique can be found in the literature (13).

2.2.2. Nuclear reaction analysis. The general scheme for NRA is

$$m_1 + m_2 \rightarrow m_3 + m_4 + Q,$$

where a particle of mass m_1 is incident on a target atom of mass m_2, giving an emitted particle of mass m_3 and a residual nucleus of mass m_4. Q is the energy released in the process. For an incident beam energy E_1 and an ejected particle energy E_3 with a scattering angle of θ, conservation of momentum and energy gives

$$E_3 = \frac{E_1 m_1 m_3}{(m_3+m_4)^2}\left\{2\cos^2\theta + \frac{m_4}{m_1 m_3}(m_3+m_4)\left(\frac{Q}{E_1}+1-\frac{m_1}{m_4}\right) + 2\cos\theta\sqrt{\cos^2\theta + \frac{m_4(m_3+m_4)}{m_1 m_3}\left(\frac{Q}{E_1}+1-\frac{m_1}{m_4}\right)}\right\}.$$

To detect carbon in the FCC samples, the $^{12}C(d, p)^{13}C$ nuclear reaction was used, which is exothermic by 2.73 MeV. The incident beam was 1.4 MeV, inducing the carbon-12 to carbon-13 nuclear reaction. With a scattering angle of approximately 180°, this results in the emission of a 3.2 MeV proton, the production rate of which is used as a measure of the amount of carbon present. The information depth of the technique depends on the sample matrix, but is of the order of a few microns.

The cross section for the $^{12}C(d, p)^{13}C$ reaction has a resonance at 1.28 MeV. Therefore, by using a beam energy of 1.4 MeV, the signal from the surface is reduced relative to that from immediately below the outer surface of the sample. This has the advantage of minimising the effect on the signal of carbon buildup during the analysis. Under these conditions, the probe depth is approximately 3 μm.

The deuteron beam also produces a PIXE spectrum which, although not sufficiently intense for quantitative work, was used to check the correct alignment between the NRA and proton-PIXE data.

The determination of carbon by NRA was quantified using a reference signal from a standard sample of 100% active carbon particles also embedded in waterglass. As for PIXE, further details on the technique and the necessary reference data can be found in the literature (14, 15).

The combination of the two techniques allows the distribution of the carbon and other elements to be measured with good spatial registration, leading to the possibility of the examination of spatial correlations between elements (allowing for the differences in information depth).

3. RESULTS AND DISCUSSION

3.1. Overall Composition Distributions

Initial experiments were performed with a defocused beam to give a survey of the range of possible compositions over 24 particles chosen at random. Spectra were acquired for all the particles examined and quantified using the Gupix software. It is well known that Ni adsorbed from the feedstock onto the catalyst particle during the FCC process is immobile, and therefore it has been suggested to use the Ni concentration as a measure of the relative age of

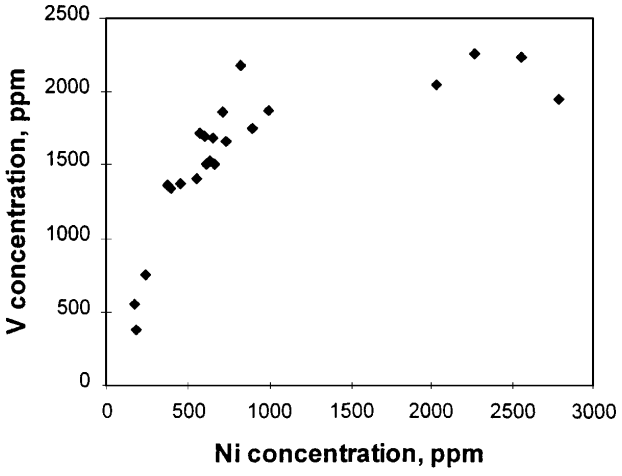

FIG. 3. Scatter plot of V vs Ni concentrations in ppm for the FCC particles studied.

the particle (4). Figure 3 shows that the vanadium concentration on a particular particle initially increases with age, but tends towards a saturation value, indicating a redistribution of vanadium due to its mobility (1, 4). This figure is superficially similar to that obtained by SIMS by Leta *et al*. (16). However, the scatter is somewhat lower, and it is likely that the accuracy of the composition scales is higher in comparison to the SIMS results. The plot of V versus Ni concentrations determined by PIXE shown in Fig. 3 was used to differentiate old, young, and middle-aged FCC particles from the sample of 24 measured. Of these, one old, one middle-aged, and one young particle were selected for detailed micro-analysis.

Scatter plots were also made of the Fe versus Ni and C (from NRA) versus Ni distributions. The Fe versus Ni distribution shown in Fig. 4 exhibits a very similar behaviour to

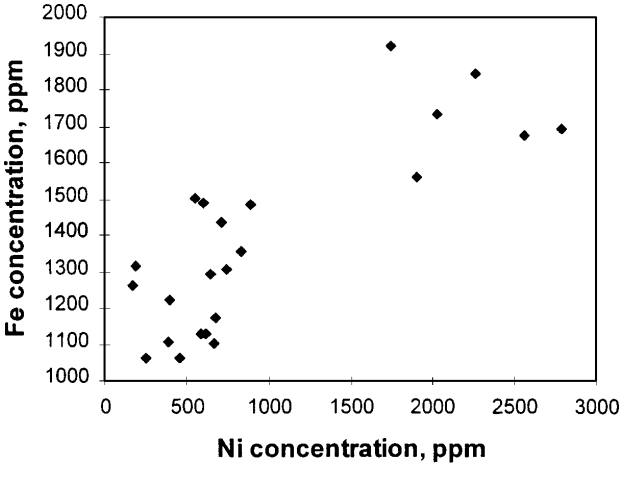

FIG. 4. Scatter plot of Fe vs Ni concentrations in ppm for the FCC particles studied.

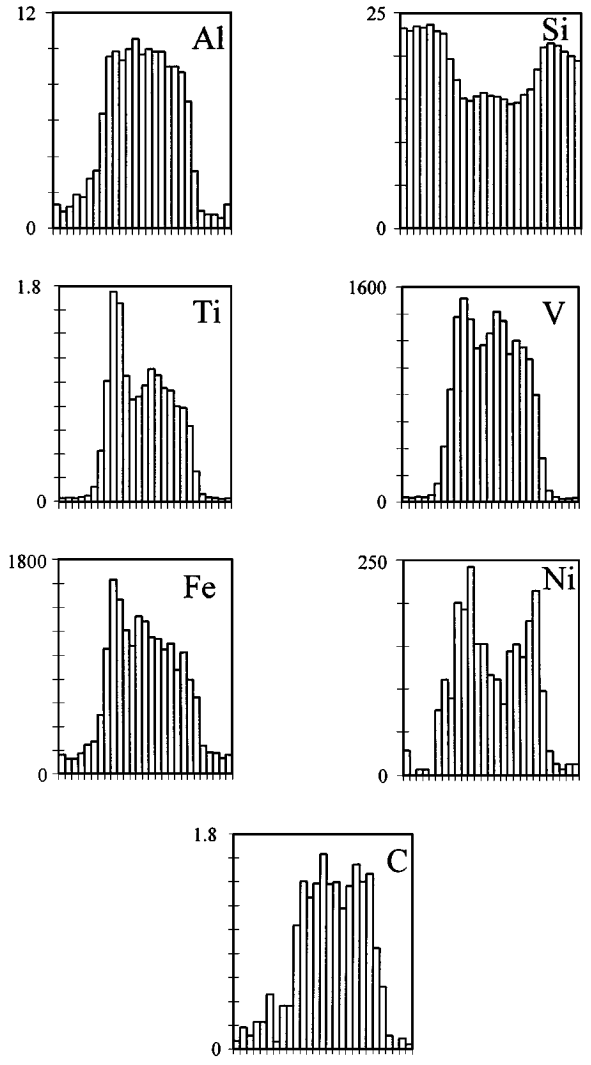

FIG. 5. PIXE line-scans for Al, Si, Ti, V, Fe, and Ni, and NRA line scan for C for the young FCC particle. PIXE line scans for Al, Si, Ti, V, Fe, and Ni, and NRA line scan for C across the young FCC particle. Concentrations are in wt% for Al, Si, Ti, and C, and ppm for V, Fe, and Ni. Data points are 10 μ apart over a scan of approximately 250 μ.

the V versus Ni distribution, only with rather more random variation. Iron is not only deposited from the feedstock, but may also be present as an impurity in the starting ingredients (clay) in the fresh catalyst, thereby accounting for the increased scatter compared with the V versus Ni plot. The C versus Ni distribution showed no systematic trend with Ni concentration; instead, the C level appeared to vary randomly between approximately 0.7 and 1.4 wt%. The overall carbon level is expected to be determined by the amount of active (zeolite) phase present, which decreases with time due to hydrothermal deactivation, and the amount of metals present, which increases with time. It is likely that these two effects cancel out to a certain extent, resulting in the observed relatively small inter-particle variability in the carbon level.

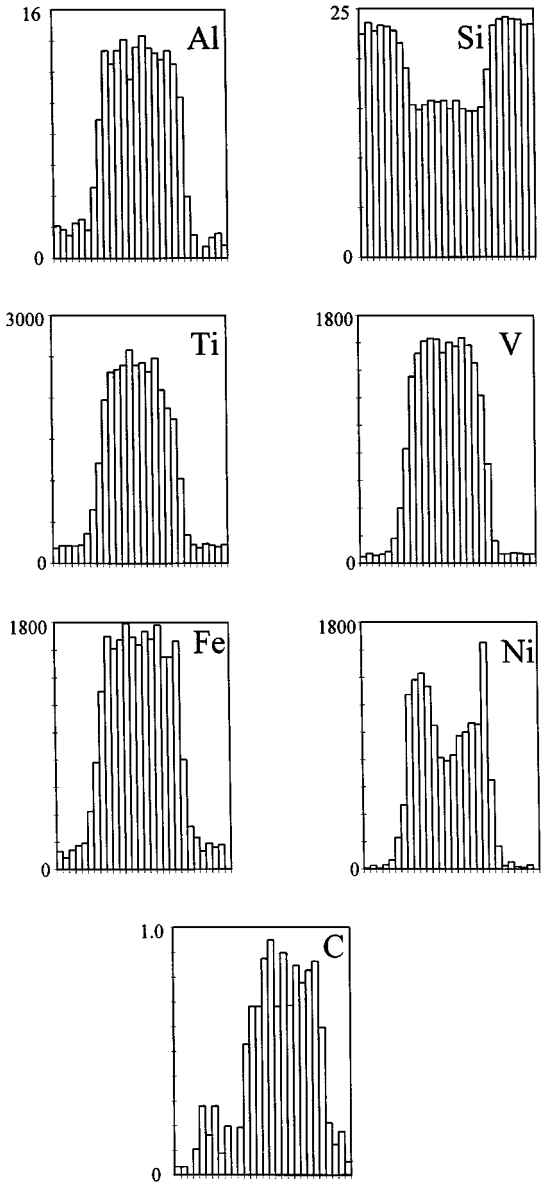

FIG. 6. PIXE line-scans for Al, Si, Ti, V, Fe, and Ni, and NRA line scan for C for the middle-aged FCC particle. PIXE line scans for Al, Si, Ti, V, Fe, and Ni, and NRA lines scan for C across the middle-aged FCC particle. Concentrations are in wt% for Al, Si, and C, and in ppm for Ti, V, Fe, and Ni. Data points are 10 μm apart over a total scan of approximately 250 μm.

3.2. Line Scans

Line scans were made across cross sections of catalyst particles by sweeping the deuteron or proton beam and measuring the X ray and particle energy spectra as a function of beam position. A microscope and CCD camera were used to ensure that the line across the catalyst particle was in the same position for both beams. The 2.5 MeV PIXE line profiles of Al, Si, Ti, V, Fe, and Ni, and the NRA line scan of C for the young, middle-aged, and old particles are shown in Figs. 5, 6, and 7, respectively. To establish baselines, all line scans were started approximately 30–40 μm away from the particle on the waterglass mount medium and continued for a similar distance on the other side of the particle. PIXE line scans for Al, Si, and Ti were also made using the 1.4 MeV NRA deuteron beam. These had relatively poor statistics, due to the lower PIXE cross section at this energy of 0.7 MeV per nucleon, compared to the value of 2.5 MeV used for the better quality data. They were used for checking the alignment between the PIXE and NRA scans, and are not shown here.

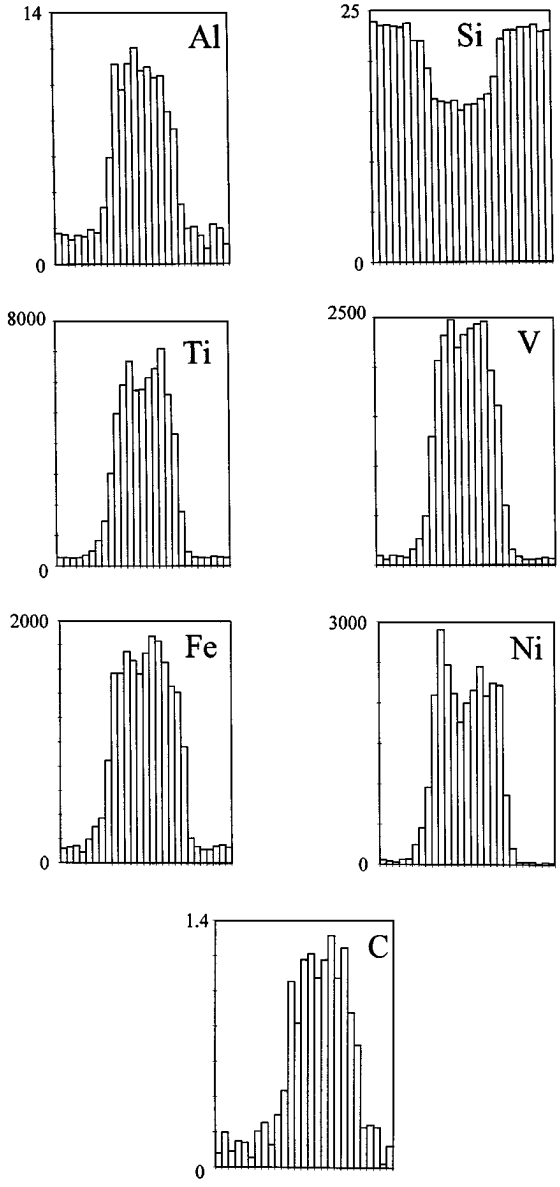

FIG. 7. PIXE line scans for Al, Si, Ti, V, Fe, and Ni, and NRA line scan for C for the old FCC particle. PIXE line scans for Al, Si, Ti, V, Fe, and Ni, and NRA lines scan for C across the old FCC particle. Concentrations are in wt% for Al, Si, and C, and in ppm for Ti, V, Fe, and Ni. Data points are 10 μm apart over a total scan of approximately 250 μm.

TABLE 1

Summary of Composition Data Obtained from Line Scans by PIXE and NRA across Old, Young, and Middle Aged Particles

	Young		Middle		Old	
Element	Max	Min	Max	Min	Max	Min
Al (%)	10.5	9.0	14.3	11.3	12.1	9.8
Si (%)	15.8	14.1	15.5	14.6	16.2	15.1
Ti (ppm)	17700	8000	2580	2010	7210	5770
V (ppm)	1520	1100	1640	1540	2490	2200
Fe (ppm)	1630	870	1790	1560	1880	1560
Ni (ppm)	240	80	1660	790	2900	1770
C (%)	1.63	1.18	0.95	0.69	1.32	0.82

For each element on each particle, every point on the line scan was quantified to give information on the range of data to be expected. A summary of the maximum and minimum compositions of the elements measured on the three particles is given in Table 1.

The variations in composition seen in Table 1 result from inter-particle variability and the effects of lifetime. Ni, Fe, and V levels tend to increase with lifetime as expected. The C level shows no great variability. The Al and Si reflect the composition of the bulk of the particle, although the Si level may be increased by absorbed embedding material. Except for the Ni, the variation between the maximum and minimum compositions is reduced with increasing lifetime. Inspection of the line scans shows that Ni is concentrated near the edges of the particles, as expected from the previous SIMS results (4), and that the other elements tend to be more uniformly distributed, but with local variations.

3.3. Images

Following the evaluation of the line-scan data, two-dimensional images showing compositional variations across the young and middle-aged samples were made. Data acquisition was rather time-consuming, requiring 6 h for the NRA measurement of the carbon distribution and a further

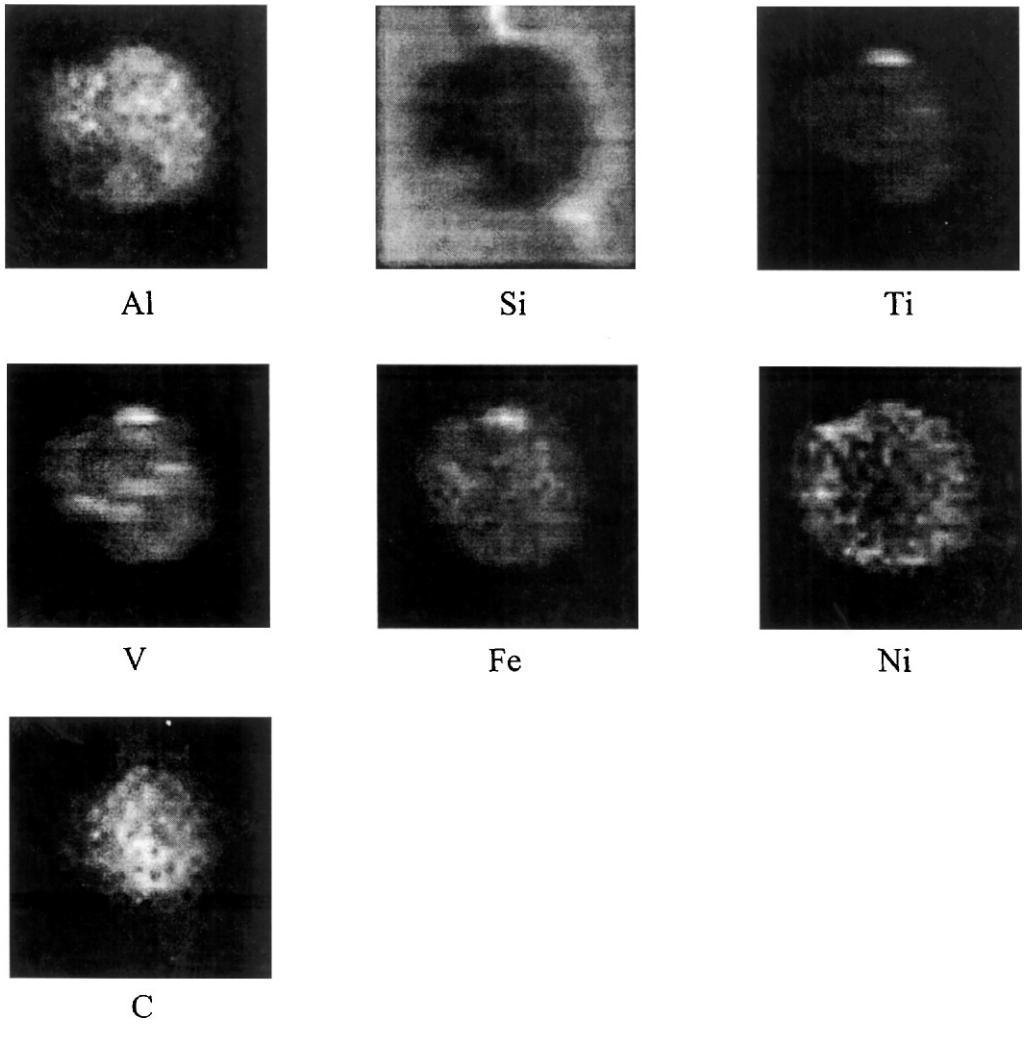

FIG. 8. PIXE images for Al, Si, Ti, V, Fe, and Ni, and NRA image for C for the young FCC particle.

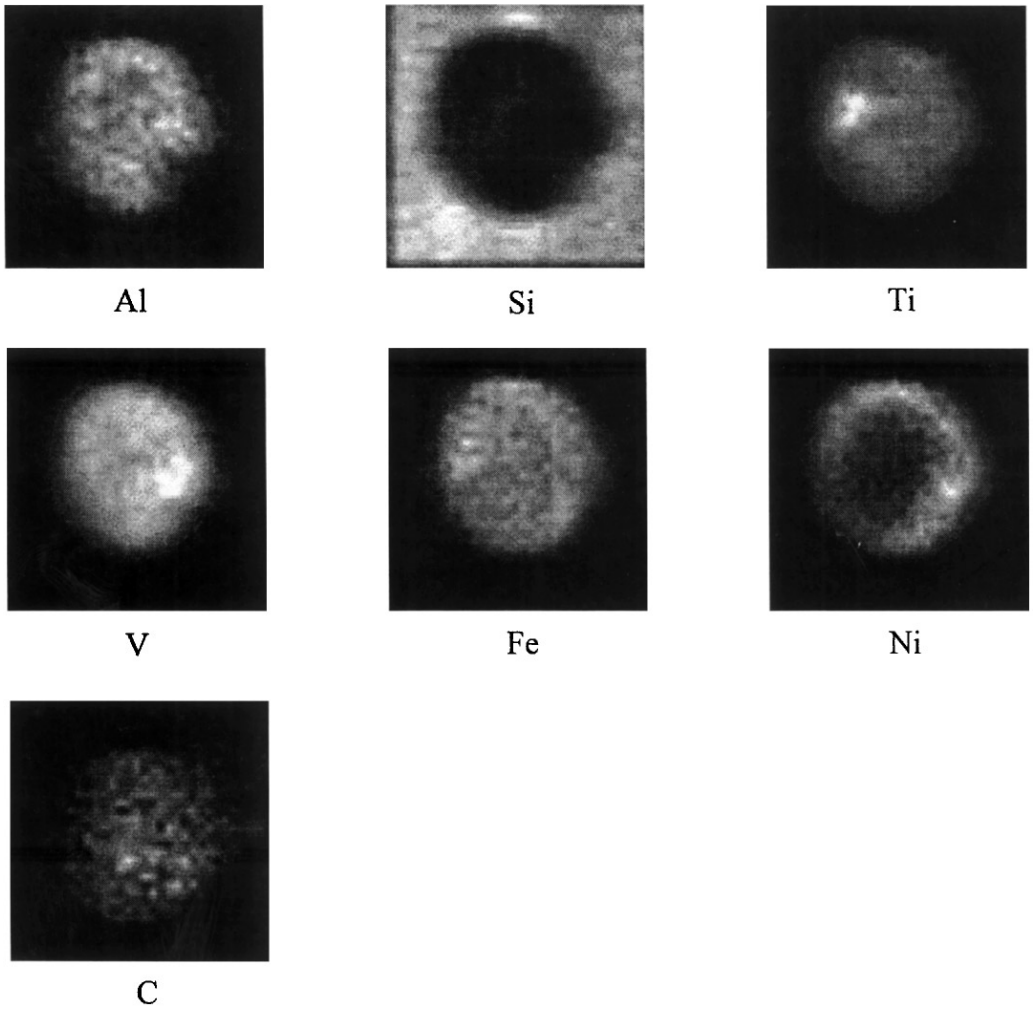

FIG. 9. PIXE images for Al, Si, Ti, V, Fe, and Ni, and NRA image for C for the middle-aged FCC particle.

3 h for the PIXE data on the other elements investigated. The resulting images, acquired over a 32×32 pixel grid, are shown in Figs. 8 and 9 for the young and middle-aged particles, respectively. In each case, the proton-induced PIXE images for Al, Si, Ti, V, Fe, and Ni, and the deuteron-NRA image for C are shown. PIXE images induced by the 1.4 MeV deuteron beam were also acquired but, as was the case for the line scans, they served only to confirm the alignment between the proton and deuteron beams and are not shown here. The figures are grey-scale-coded with the brightness of each pixel proportional to the amount of each element detected.

Inspection of these images shows that for the young particle the Al and Si images are anti-correlated. This is expected as they form major components of the particle matrix. There is a clear correlation between the Ti and V images, also expected, as Ti is used as a trap for V. The Fe may have some correlation with the Ti and V. Part of this apparent correlation may arise from Fe from the feedstock; however, the presence of Fe as an impurity in the clay would tend to obscure this correlation. Ni is confined to the outermost 10 μm or so of the particle. It originates from the feedstock and remains where it is first deposited on the particle, probably due to the lower mobility of its high melting point oxides, compared to, for example, the vanadium oxides which are more mobile.

In the middle-aged particle the Al and Si still show an anti-correlation, but the other correlations appear to have become smoothed out with age. Ni is still confined to the outer layers of the particle and may possibly show some anti-correlation with C. Such an anti-correlation may arise from the tendancy of Ni to promote hydrogenolysis of coke, but this is not clear from the image.

Despite the fact that the commercial unit from which the sample was taken was processing a relatively heavy feedstock (4 wt% CCR), the carbon appears to be relatively uniformly distributed across the particle. This seems to indicate that even the large bulky molecules present in the FCC feed

can be cracked on the external surface of the FCC particle and the lighter fragments so formed are further cracked in the interior of the particle. Also carbon shows no obvious correlation with any of the other elements. This is not surprising as carbon formation is an intricate process influenced not only by the metals, but also by the nature and amount of the acid (active) ingredients present.

To obtain further insight into possible spatial and chemical correlations within the particles, principal component analysis was used. This was carried out using the three sets of line scans from the young, middle-aged, and old particles, and separately using a selection of line scans extracted from the image data from either the young or middle-aged particle. The results confirmed the positive correlation between Ti, V, and Fe, and also showed an anti-correlation between these three and Ni. An anti-correlation between the matrix elements Si and Al was also seen. However, it is important to note that the deviations in the amount of correlation seen between the line scans for the young, middle-aged, and old particles was also seen when comparing line scans across the same particle. This means that with this limited data set it is not possible to distinguish between the effects of age and the natural variability within a particle.

4. CONCLUSIONS

This work has shown that nuclear beam techniques can be used to give quantitative spatially resolved information on the distribution of elements, including carbon, within catalyst particles.

Carbon is found to be quite uniformly distributed through the particles examined. Unlike Ni, it is not confined to the outer surface of the particles, which may indicate that the incoming bulky molecules containing nickel are cracked into smaller fragments at the external surface of the FCC particle, leaving nickel at the outer rim of the particle. Spatial correlations between elements within the used FCC catalyst particles have been seen and are consistent with observations reported previously using SIMS. However, as expected, no general relationship between the metal elements and carbon concentrations could be found.

Key to this work has been the successful exploitation of the carbon-free sample embedding technique involving waterglass. Analysis of the samples resulting from the waterglass embedding is not limited to micro-PIXE or NRA and may be more widely applicable in surface analysis and microscopy of catalyst and other materials.

ACKNOWLEDGMENTS

Discussions with Dr. W. Koot and Dr. O. E. de Noord (SRTCA) and the assistance of K. Wiederspahn (VU Amsterdam) are gratefully acknowledged.

REFERENCES

1. Peters, A. W., Instrumental methods of FCC catalyst characterisation, *in* "Studies in Surface Science and Catalysis," (J. S. Magee and M. M. Mitchell, Jr., Eds.), Vol. 76. Elsevier, Amsterdam, 1993.
2. Chao, K. J., Lin, L. H., Ling, Y. C., Hwanf, J. F., and Hou, L. Y., *Appl. Catal. A* **121**, 217 (1995).
3. Lampert, J. K., Koermer, G. S., Macaoay, J. M., Chabal, J. M., and Levi-Setti, R., *Appl. Surf. Sci.* **55**, 149 (1992).
4. Kugler, E. L., and Leta, D. P., *J. Catal.* **109**, 387 (1988).
5. Altomare, C. A., Koermer, G. S., Martins, E., Schubert, P. F., Suib, S. L., and Willis, W. S., *Appl. Catal.* **45**, 291 (1988).
6. Wormsbecher, R. F., Peters, A. W., and Maselli, J. M., *J. Catal.* **100**, 130 (1986).
7. Suib, S. L., Borgstedt, E. V., Cao, H., and Occelli, M. L., *in* "Studies in Surface Science and Catalysis" (C. H. Bartholomew and J. B. Butt, Eds.) Vol. 68. Elsevier, Amsterdam, 1991.
8. Gallezot, P., Leclercq, C., Guisnet, M., and Magnoux, P., *J. Catal.* **114**, 100 (1988).
9. Turlier, P., Forissier, M., Rivault, P., Pitault, I., and Bernard, J. R., Catalyst fouling by coke from vacuum gas oil in fluid catalytic cracking reactors, *in* "Fluid catalytic cracking III" (M. L. Occelli and P. O'Connor, Eds.), ACS Symp. Ser., Vol. 571, p. 98. Am. Chem. Soc. Washington, 1994.
10. Vis, R. D., On the determination of carbon using charged particle accelerators *Nucl. Instrum. Methods Phys. Res. B* **66**, 139 (1992).
11. Vis, R. D., Kramer, J. L. A. M., Tros, G. H. J., van Langeveld, F., and Maks, L., *Nucl. Instrum. Methods Phys. Res. B* **77**, 41 (1993).
12. Maxwell, J. A., Campbell, J. L., and Teesdale, W. J., *Nucl. Instrum. Methods Phys. Res. B* **43**, 218 (1989).
13. Johansson, S. A. E., and Cambell, J. L., "PIXE: A Novel Technique for Elemental Analysis." Wiley, Chichester, UK, 1988.
14. Thomas, J. P., and Cachard, A., "Materials Characterisation Using Ion Beams." Plenum, New York, 1978.
15. Mayer, J. W., and Rimini, E., "Ion Beam Handbook for Material Analysis," Academic Press, New York, 1977.
16. Leta, D. P., Lamberti, W. A., Varady, W. A., and Clark, T. E., *in* "Secondary Ion Mass Spectrometry—SIMS VIII" (A. Benninghoven, K. T. F. Janssen, J. Tümpner, and H. W. Werner, Eds.), p. 541, Wiley, Chichester, 1992.